Latin American Journal of Solids and Structures
www.lajss.org

# Aerothermoelastic Analysis of Functionally Graded Plates Using Generalized Differential Quadrature Method

**Abstract**

In the present paper, the aerothermoelastic behavior of Functionally Graded (FG) plates under supersonic airflow is investigated using Generalized Differential Quadrature Method (GDQM). The structural model is considered based on the classical plate theory and the von Karman strain-displacement relations are utilized to involve the nonlinear behavior of the plate. To consider the supersonic aerodynamic loads on the plate, the first order piston theory is applied. The material properties of the FG panel are assumed to be temperature independent and alter in the thickness direction according to a power law distribution. The temperature distribution on the surface of the plate is assumed to be constant and in the thickness direction is obtained by one-dimensional steady conductive heat transfer equation. The discretized governing equations via GDQM are solved by the fourth order Runge-Kutta method. Comparison of the obtained results with those available in literature confirms the accuracy and ability of the GDQM to perform the aerothermoelastic analysis of FG plates. Also, the effect of some important parameters such as Mach number, in-plane thermal load, plate aspect ratio and volume fraction index on the plate aerothermoelastic behavior is examined.

**Keywords**

Differential Quadrature Method, Aerothermoelastic, Functionally Graded Material, Stability boundary.

**H. Shahverdi** [a]
**V. Khalafi** [b]
**S. Noori** [c]

[a, b, c] Department of Aerospace Engineering and Center of Excellence in Computational Aerospace Engineering, Amirkabir University of Technology, Tehran, Iran

Author email:
[a] Corresponding author,
h_Shahverdi@aut.ac.ir
[b] v.kh@aut.ac.ir
[c] S_noori@aut.ac.ir

http://dx.doi.org/10.1590/1679-78252072

Received 22.04.2015
In revised form 28.10.2015
Accepted 20.01.2016
Available online 17.02.2016

## 1 INTRODUCTION

The lifting surfaces and panels of space re-entry vehicles and high-speed aircrafts are exposed to combined effects of aerodynamic, thermodynamic, inertial, and elastic forces. One of the key factors in the design of their outer skins is the aerothermoelastic considerations. In this regard many researches have been performed.

The first studies on the flutter behavior of a panel can be traced back to the works of Houbolt (1958), Bolotin (1963) and Dowell (1966, 1975). Schaeffer and Heard (1965) studied aeroelastic response of a flat panel exposed to a nonlinear temperature distribution with simply support boundary conditions. Xue and Mei (1993a) investigated the nonlinear flutter response of isotropic panels under thermal effects using FEM. To account for structural nonlinearity, von Karman's large detion plate theory was considered. They studied the effects of nonuniform temperature distribution, panel aspect ratio, and boundary conditions on the flutter behaviors of rectangular and triangular panels. Also, Xue and Mei (1993b) considered the fatigue life of isotropic panels in frequency domain using FEM and investigated the effect of dynamic pressure and temperature on the fatigue life of a panel.

In the modern structures, a new material with desired mechanical and strength properties is generated by combining of different material layers. Thus, Isotropic materials have been replaced by composite materials. In the recent decades, Functionally Graded Materials (FGMs) have attracted considerable attention as materials for various advanced purposes. Functionally graded materials are a new type of inhomogeneous materials and advanced composites. A functionally graded material is usually a combination of two materials or phases that have gradual transition of properties from one side of sample to another side. This gradual transition allows the thermo-mechanically interface problems in a composite structure such as sharp local stress concentration, delamination and weak thermal resistance, can be impressively decreased (Miyamoto et al., 1999). Across the consecutive development of FGMs, there have been many research works as follows. Praveen and Reddy (1998) investigated the static and dynamic response of functionally graded plates using a plate finite element that accounted for the effects of the transverse shear strains, rotary inertia and the moderately large rotations in the von Karman sense. They showed that the response of the plates with material properties between those of the ceramic and metal is not intermediate to the responses of the ceramic and metal plates. Javaheri and Eslami (2002) derived stability equations of a rectangular functionally graded plate using with the classical plate theory. Sohn and Kim (2008) analyzed structural stability of functionally graded panels under simultaneous thermal and aerodynamic loads. In this work, thermal post-buckling behaviors and stability boundaries for clamped and simply support FG panels with uniform temperature gradients were studied**.** Sohn and Kim (2009) studied the aerothermoelastic instability of FGM panels in supersonic flow and showed the effects of the volume fraction distributions, temperature changes, aerodynamic pressures and the boundary conditions on the panel flutter**.** Navazi and Haddadpour (2011) analyzed the nonlinear flutter behavior and stability boundaries of isotropic and FGM plates in supersonic airflow, and showed that under real flight conditions and using coupled model, the aerodynamic heating is very severe and the type of instability is divergence. Janghorban and Zare (2011) examined the vibration analysis of a functionally graded plate with cutouts and skew boundary. In this work, the role of different parameters such as cutout size, type of loading and different boundary conditions on the vibration of the plate was reported. Taj and Chakrabarti (2013) investigated a finite element formulation based on Reddy's higher order theory to investigate the dynamic response of a FG skew shell.

So far, different analysis techniques have been used for panel flutter studies. However, the methods having less computational complexity (and effort) and greater accuracy are of most interest to researchers. One of them is DQM which first presented by Bellman and Casti (1971). The

main idea behind the DQM is that the derivative of a function with respect to a space variable at a given point is approximated as a weighted linear sum of the function values at all discrete points along the domain of that variable.

The DQM has been applied to solve various structural elements such as beams, plates and shells. Bert et al. (1988) applied the DQM to investigate static and dynamic response of structures for the first time, and afterwards it was improved by Bert and Malik (1996). Also, Bert et al. (1989) used DQM for composite plates for the first time and analyzed nonlinear bending of orthotropic rectangular plates. Then, Shu and Richards (1992) presented the GDQM to simplify the computation of the weighting coefficients. Shu and Wang (1999) applied GDQM for vibration analysis of a rectangular plate with combined and non-uniform boundary conditions. Fazelzadeh et al. (2007) investigated the vibration of a rotating thin walled-blade made of functionally graded materials operating under high temperature supersonic gas flow with DQM. Talebitooti et al. (2013) presented the effects of boundary conditions and axial loading on the frequency characteristics of rotating laminated conical shells with orthogonal stiffeners using GDQM.

This paper extends the application of the DQM to aerothermoelastic analysis of a flat plate in supersonic flow. In this regard the governing differential aeroelastic equations of a FG plate as first discretized using GDQM and then aerothermoelastic response of the plate is studied by the fourth order Runge-Kutta method. To demonstrate the accuracy and fidelity of the GDQM, the dynamic stability boundaries of the plate are validated with available results presented by other researchers. Also, the effects of some important parameters such as Mach number, in-plane thermal load, plate aspect ratio and volume fraction index on the plate aerothermoelastic behavior are investigated.

## 2 FORMULATION

### 2.1 Structural Model

A plate with length $a$, width $b$, and thickness $h$ made up of a mixture of ceramic and metal is considered. The airflow is assumed in the $x$-direction. Volume fraction of the functionally graded material varies continuously through the plate thickness according to a simple power law (Javaheri and Eslami, 2002). Hence:

$$V_m = \left( \frac{z + h/2}{h} \right)^n \tag{1}$$

$$\left( V_m + V_c = 1 \right) \tag{2}$$

where $z$ is the coordinate in the thickness direction with origin at the plate mid-surface and $n$ is the volume fraction index. Thus, the material properties of the functionally graded plate can be expressed as

$$P_{eff} = P_m V_m + P_c V_c \tag{3}$$

$$P_{eff} = \left(P_c - P_m\right)\left(\frac{z+h/2}{h}\right)^n + P_m \tag{4}$$

where subscripts $c$ and $m$ refer to ceramic and metal, respectively, and $P_{eff}$ is the effective material properties of the plate corresponding to the modulus of elasticity $(E)$, Poisson's ratio $(\upsilon)$, density $(\rho)$ and thermal coefficient expansion$(\alpha)$.

Based on the Classical Plate Theory (CPT), the displacement field of the plate is:

$$\begin{aligned} u(x,y,z,t) &= u_0(x,y,t) - z\frac{\partial w_0(x,y,t)}{\partial x} \\ v(x,y,z,t) &= v_0(x,y,t) - z\frac{\partial w_0(x,y,t)}{\partial y} \\ w(x,y,z,t) &= w_0(x,y,t) \end{aligned} \tag{5}$$

where $u_0$ and $v_0$ are the in-plane displacement components, and $w_0$ is the out-of-plane displacement component measured from the plate's mid-plane.

According to the von Karman nonlinear strain-displacement relations, the nonlinear strains are defined as:

$$\{\varepsilon\} = \{\varepsilon^0\} + z\{k\} \tag{6}$$

where $\varepsilon^0$ and $k$ are the mid-plane membrane and bending strain vectors, respectively, which can be defined as follows:

$$\{\varepsilon^0\} = \begin{Bmatrix} \varepsilon_{xx}^{\ 0} \\ \varepsilon_{yy}^{\ 0} \\ \varepsilon_{xy}^{\ 0} \end{Bmatrix} = \begin{Bmatrix} u_{0,x} \\ v_{0,y} \\ u_{0,y} + v_{0,x} \end{Bmatrix} + \frac{1}{2}\begin{Bmatrix} w_{0,x}^2 \\ w_{0,y}^2 \\ 2w_{0,x}w_{0,y} \end{Bmatrix} \tag{7}$$

$$\{k\} = \begin{Bmatrix} k_{xx} \\ k_{yy} \\ k_{xy} \end{Bmatrix} = \begin{Bmatrix} -w_{xx} \\ -w_{yy} \\ -2w_{xy} \end{Bmatrix} \tag{8}$$

The thermoelastic constitutive equations of the FG panels are:

$$\begin{Bmatrix} \sigma_{xx} \\ \sigma_{yy} \\ \sigma_{xy} \end{Bmatrix} = \begin{bmatrix} Q_{11} & Q_{12} & 0 \\ Q_{12} & Q_{22} & 0 \\ 0 & 0 & Q_{66} \end{bmatrix} \begin{Bmatrix} \varepsilon_{xx} - \alpha\left(z,T\right)\Delta T(z) \\ \varepsilon_{xx} - \alpha\left(z,T\right)\Delta T(z) \\ \varepsilon_{xy} \end{Bmatrix} \tag{9}$$

$$\Delta T(z) = T(z) - T_0 \tag{10}$$

where $T_0$, $T(z)$ and $\alpha(z,T)$ are reference temperature, temperature distribution in the plate thickness direction and thermal expansion coefficient, respectively. $Q_{ij}$ are the elements of material constant matrix and defined by

$$Q_{11} = Q_{22} = \frac{E(z)}{1-\nu(z)^2}$$
$$Q_{12} = \frac{\nu(z)E(z)}{1-\nu(z)^2} \tag{11}$$
$$Q_{66} = \frac{E(z)}{2\left(1+\nu(z)\right)}$$

where $E(z)$ is the elastic modulus of a FG panel.

In-plane force resultant and out-of-plate moment resultant are obtained as follows:

$$\begin{Bmatrix} \mathbf{N} \\ \mathbf{M} \end{Bmatrix} = \begin{bmatrix} \mathbf{A} & \mathbf{B} \\ \mathbf{B} & \mathbf{D} \end{bmatrix} \begin{Bmatrix} \{\varepsilon^0\} \\ \{k\} \end{Bmatrix} - \begin{Bmatrix} \mathbf{N}^T \\ \mathbf{M}^T \end{Bmatrix} \tag{12}$$

Here, $\mathrm{N}^T$ and $\mathrm{M}^T$ are the thermal in-plane force and moment resultant vectors. Thus

$$\left(\mathbf{N}^T, \mathbf{M}^T\right) = \int_{-\frac{h}{2}}^{\frac{h}{2}} (1, z)\mathbf{Q} \begin{Bmatrix} \alpha(z) \\ \alpha(z) \\ 0 \end{Bmatrix} \Delta T(z) dz \tag{13}$$

while A, B and D are extension, bending–extension coupling, and bending stiffness and are given as follows:

$$\mathbf{A} = \begin{bmatrix} A_{11} & A_{12} & 0 \\ A_{12} & A_{22} & 0 \\ 0 & 0 & A_{66} \end{bmatrix}, \mathbf{B} = \begin{bmatrix} B_{11} & B_{12} & 0 \\ B_{12} & B_{22} & 0 \\ 0 & 0 & B_{66} \end{bmatrix}, \mathbf{D} = \begin{bmatrix} D_{11} & D_{12} & 0 \\ D_{12} & D_{22} & 0 \\ 0 & 0 & D_{66} \end{bmatrix} \tag{14}$$

$$(A_{ij}, B_{ij}, D_{ij}) = \int_{-\frac{h}{2}}^{\frac{h}{2}} Q_{ij}(1, z, z^2) dz \tag{15}$$

### 2.2 Aerodynamic Model

According to the first order piston theory (Dowell, 1975), the aerodynamic pressure, may be expressed as

$$\Delta p = \frac{2q}{\sqrt{M^2-1}} \left( \frac{1}{U_\infty} \left( \frac{M^2-2}{M^2-1} \right) \frac{\partial w}{\partial t} + \frac{\partial w}{\partial x} \right) \tag{16}$$

where $q$, $M$ and $U_\infty$ represent the dynamic pressure, Mach number, and the free stream velocity, respectively. The linear piston theory is valid for $\sqrt{2} < M < 5$ (Mei et al., 1999).

### 2.3 Temperature Distribution

The temperature distribution on the surface of the plate is assumed to be constant while in the thickness direction it is considered to be variable and may be obtained by solving the one-dimensional Fourier equation of the heat conduction, which is

$$\frac{d}{dz}\left[K(z)\frac{dT}{dz}\right]=0\ , \qquad \begin{cases} T=T_c & at \quad z=\dfrac{h}{2} \\ T=T_m & at \quad z=-\dfrac{h}{2} \end{cases} \tag{17}$$

$T_m$ and $T_c$ are the temperature of the lower and upper surfaces of the panel, and temperature distribution in the plate thickness direction is obtained by means of polynomial series (Javaheri and Eslami, 2002) and given as follows:

$$T(z)=T_m+(T_c-T_m)\Gamma(z) \tag{18}$$

where

$$\begin{aligned}\Gamma(z)=&\frac{1}{C}\left(\frac{z}{h}+\frac{1}{2}\right)-\frac{(K_c-K_m)}{K_m(n+1)}\left(\frac{z}{h}+\frac{1}{2}\right)^{(n+1)}+\frac{(K_c-K_m)^2}{{K_m}^2(2n+1)}\left(\frac{z}{h}+\frac{1}{2}\right)^{(2n+1)}\\&-\frac{(K_c-K_m)^3}{{K_m}^3(3n+1)}\left(\frac{z}{h}+\frac{1}{2}\right)^{(3n+1)}+\frac{(K_c-K_m)^4}{{K_m}^4(4n+1)}\left(\frac{z}{h}+\frac{1}{2}\right)^{(4n+1)}-\frac{(K_c-K_m)^5}{{K_m}^5(5n+1)}\left(\frac{z}{h}+\frac{1}{2}\right)^{(5n+1)}\end{aligned} \tag{19}$$

$$C=1-\frac{(K_c-K_m)}{K_m(n+1)}+\frac{(K_c-K_m)^2}{{K_m}^2(2n+1)}-\frac{(K_c-K_m)^3}{{K_m}^3(3n+1)}+\frac{(K_c-K_m)^4}{{K_m}^4(4n+1)}-\frac{(K_c-K_m)^5}{{K_m}^5(5n+1)} \tag{20}$$

### 2.4 Equations of Motion

By means of the extended Hamilton's principle, the nonlinear governing equations of motion can be obtained. In the absence of surface shearing forces, body moments and inertial forces in the $x$ and $y$ directions, the aeroelastic equations of a FG plate are (Bert et al., 1989)

$$\begin{aligned}&N_{xx,x}+N_{xy,y}=0\\&N_{xy,x}+N_{yy,y}=0\\&M_{xx,xx}+2M_{xy,xy}+M_{yy,yy}+N_{xx}\frac{\partial^2 w}{\partial x^2}+2N_{xy}\frac{\partial^2 w}{\partial x\partial y}+N_{yy}\frac{\partial^2 w}{\partial y^2}+\Delta p_\infty=I_0\ddot{w}\end{aligned} \tag{21}$$

where

$$I_0 = \int_{-h/2}^{h/2} \rho(z) dz \tag{22}$$

By substituting the Eqs. (9) and (12) into Eq. 21, the equations of motion are obtained as follows:

$$A_{11}\frac{\partial \varepsilon_{xx}}{\partial x} + A_{12}\frac{\partial \varepsilon_{yy}}{\partial x} + B_{11}\frac{\partial k_{xx}}{\partial x} + B_{12}\frac{\partial k_{yy}}{\partial x} + A_{66}\frac{\partial \varepsilon_{xy}}{\partial y} + B_{66}\frac{\partial k_{xy}}{\partial y} = 0 \tag{23}$$

$$A_{12}\frac{\partial \varepsilon_{xx}}{\partial y} + A_{22}\frac{\partial \varepsilon_{yy}}{\partial y} + B_{12}\frac{\partial k_{xx}}{\partial y} + B_{22}\frac{\partial k_{yy}}{\partial y} + A_{66}\frac{\partial \varepsilon_{xy}}{\partial x} + B_{66}\frac{\partial k_{xy}}{\partial x} = 0 \tag{24}$$

$$\begin{aligned} &B_{11}\frac{\partial^2 \varepsilon_{xx}}{\partial x^2} + B_{12}\frac{\partial^2 \varepsilon_{yy}}{\partial x^2} + D_{11}\frac{\partial^2 k_{xx}}{\partial x^2} + D_{12}\frac{\partial^2 k_{yy}}{\partial x^2} + B_{12}\frac{\partial^2 \varepsilon_{xx}}{\partial y^2} + \\ &B_{22}\frac{\partial^2 \varepsilon_{yy}}{\partial y^2} + D_{12}\frac{\partial^2 k_{xx}}{\partial y^2} + D_{22}\frac{\partial^2 k_{yy}}{\partial y^2} + 2B_{66}\frac{\partial^2 \varepsilon_{xy}}{\partial x \partial y} + 2D_{66}\frac{\partial^2 k_{xy}}{\partial x \partial y} + \\ &N_{xx}\frac{\partial^2 w}{\partial x^2} + 2N_{xy}\frac{\partial^2 w}{\partial x \partial y} + N_{yy}\frac{\partial^2 w}{\partial y^2} + \Delta p_\infty = I_0 \ddot{w} \end{aligned} \tag{25}$$

By differentiating from Eq. (23) and Eq. (24) with respect to the variable of x and y, respectively, and summing the resultant equations, we will have

$$\begin{aligned} &A_{11}\frac{\partial^2 \varepsilon_{xx}}{\partial x^2} + A_{12}\frac{\partial^2 \varepsilon_{yy}}{\partial x^2} + B_{11}\frac{\partial^2 k_{xx}}{\partial x^2} + B_{12}\frac{\partial^2 k_{yy}}{\partial x^2} + A_{66}\frac{\partial^2 \varepsilon_{xy}}{\partial x \partial y} + B_{66}\frac{\partial^2 k_{xy}}{\partial x \partial y} \\ &+A_{12}\frac{\partial^2 \varepsilon_{xx}}{\partial y^2} + A_{22}\frac{\partial^2 \varepsilon_{yy}}{\partial y^2} + B_{12}\frac{\partial^2 k_{xx}}{\partial y^2} + B_{22}\frac{\partial^2 k_{yy}}{\partial y^2} + A_{66}\frac{\partial^2 \varepsilon_{xy}}{\partial x \partial y} + B_{66}\frac{\partial^2 k_{xy}}{\partial x \partial y} = 0 \end{aligned} \tag{26}$$

By multiplying $B_{11}$ to Eq. (25) and $A_{11}$ to Eq. (26) and substituting Eq. (25) into Eq. (26) and after some mathematical manipulations, the following equation is obtained.

$$\begin{aligned} &\frac{(D_{11}A_{11} - B_{11}^2)}{A_{11}}\frac{\partial^2 k_{xx}}{\partial x^2} + \nu\frac{(D_{11}A_{11} - B_{11}^2)}{A_{11}}\frac{\partial^2 k_{yy}}{\partial x^2} + \nu\frac{(D_{11}A_{11} - B_{11}^2)}{A_{11}}\frac{\partial^2 k_{xx}}{\partial y^2} \\ &+\frac{(D_{11}A_{11} - B_{11}^2)}{A_{11}}\frac{\partial^2 k_{yy}}{\partial y^2} + 2\left(\frac{1-\nu}{2}\right)\frac{(D_{11}A_{11} - B_{11}^2)}{A_{11}}\frac{\partial^2 k_{xy}}{\partial x \partial y} + N_{xx}\frac{\partial^2 w}{\partial x^2} + 2N_{xy}\frac{\partial^2 w}{\partial x \partial y} \\ &+N_{yy}\frac{\partial^2 w}{\partial y^2} + \Delta p_\infty = I_0 \ddot{w} \end{aligned} \tag{27}$$

The above equation can be written as

$$D_{eq}\left(\frac{\partial^4 w}{\partial x^4} + 2\frac{\partial^4 w}{\partial x^2 \partial y^2} + \frac{\partial^4 w}{\partial y^4}\right) + N_{xx}\frac{\partial^2 w}{\partial x^2} + 2N_{xy}\frac{\partial^2 w}{\partial x \partial y} + N_{yy}\frac{\partial^2 w}{\partial y^2} + \Delta p_\infty + I_0 \ddot{w} = 0 \tag{28}$$

where

$$D_{eq} = \frac{D_{11}A_{11} - B_{11}^{\ 2}}{A_{11}} \tag{29}$$

In this paper, the plate is considered to be simply supported along all edges and therefore the in-plane displacement components $\frac{\partial u}{\partial x}, \frac{\partial v}{\partial y}, \frac{\partial u}{\partial y}, \frac{\partial v}{\partial x}$ are equal to zero and based on this assumption the in-plane force resultants can be modified as follows (Dowell 1975, Miller et al., 2011):

$$\begin{aligned}
N_{xx} &= \int_0^b \int_0^a \left( A_{11}\frac{1}{2}(\frac{\partial w}{\partial x})^2 + A_{12}\frac{1}{2}(\frac{\partial w}{\partial y})^2 - B_{11}\frac{\partial^2 w}{\partial^2 x} - B_{12}\frac{\partial^2 w}{\partial^2 y} \right) dxdy - N_{xx}^{\ T} \\
N_{yy} &= \int_0^b \int_0^a \left( A_{12}\frac{1}{2}(\frac{\partial w}{\partial x})^2 + A_{22}\frac{1}{2}(\frac{\partial w}{\partial y})^2 - B_{12}\frac{\partial^2 w}{\partial^2 x} - B_{22}\frac{\partial^2 w}{\partial^2 y} \right) dxdy - N_{yy}^{\ T} \\
N_{xy} &= \int_0^b \int_0^a \left( A_{66}\frac{\partial w}{\partial x}\frac{\partial w}{\partial y} - 2B_{66}\frac{\partial^2 w}{\partial x \partial y} \right) dxdy
\end{aligned} \tag{30}$$

By substituting Eqs. (16) and (31) into Eq. (28), the aerothermoelastic equation is obtained.

$$\begin{aligned}
&D_{eq}\left( \frac{\partial^4 w}{\partial x^4} + 2\frac{\partial^4 w}{\partial x^2 \partial y^2} + \frac{\partial^4 w}{\partial y^4} \right) \\
&+\left[ \int_0^b \int_0^a \left( A_{11}\frac{1}{2}(\frac{\partial w}{\partial x})^2 + A_{12}\frac{1}{2}(\frac{\partial w}{\partial y})^2 - B_{11}\frac{\partial^2 w}{\partial x^2} - B_{12}\frac{\partial^2 w}{\partial y^2} \right) dxdy \right] \frac{\partial^2 w}{\partial x^2} \\
&+2\left[ \int_0^b \int_0^a \left( A_{66}\frac{\partial w}{\partial x}\frac{\partial w}{\partial y} - 2B_{66}\frac{\partial^2 w}{\partial x \partial y} \right) dxdy \right] \frac{\partial^2 w}{\partial x \partial y} \\
&+\left[ \int_0^b \int_0^a \left( A_{12}\frac{1}{2}(\frac{\partial w}{\partial x})^2 + A_{22}\frac{1}{2}(\frac{\partial w}{\partial y})^2 - B_{12}\frac{\partial^2 w}{\partial x^2} - B_{22}\frac{\partial^2 w}{\partial y^2} \right) dxdy \right] \frac{\partial^2 w}{\partial y^2} \\
&-N_{xx}^{\ T}\frac{\partial^2 w}{\partial x^2} - N_{yy}^{\ T}\frac{\partial^2 w}{\partial y^2} + \frac{2q_\infty}{U_\infty \beta}\left( U_\infty \frac{\partial w}{\partial x} + \frac{M^2 - 2}{M^2 - 1}\frac{\partial w}{\partial t} \right) + I_0 \ddot{w} = 0
\end{aligned} \tag{31}$$

In a supersonic regime, the coefficient of the aerodynamic damping in Eq. (31) can be approximately expressed as (Liaw and Yang, 1993)

$$\left( \frac{M^2 - 2}{M^2 - 1} \right)^2 \left( \frac{\mu}{\sqrt{M^2 - 1}} \right) \approx \frac{\mu}{M} \tag{32}$$

In order to express Eq. (31) in a non-dimensional form, the following set of dimensionless parameters is defined as follows:

$$
\begin{aligned}
W &= \frac{w}{h} & \zeta &= \frac{x}{a} \\
\eta &= \frac{y}{b} & \lambda &= \frac{2q_\infty a^3}{\beta D_m} \\
\mu &= \frac{\rho_\infty a}{\rho_m h} & \tau &= t\left(\frac{D_m}{\rho_m h a^4}\right)^{1/2} \\
R_x &= \frac{{N_{xx}}^T a^2}{D_m} & R_y &= \frac{{N_{yy}}^T b^2}{D_m}
\end{aligned}
\tag{33}
$$

By introducing the above parameters into Eq. (31), the non-dimensional form of aeroelastic equations can be obtained.

$$
\begin{aligned}
&\frac{I_0}{\rho_m h}\frac{\partial^2 W}{\partial^2 \tau}+\frac{D_{eq}}{D_m}\left(\frac{\partial^4 W}{\partial \zeta^4}+2\left(\frac{a}{b}\right)^2\frac{\partial^4 W}{\partial \zeta^2 \partial \eta^2}+\left(\frac{a}{b}\right)^4\frac{\partial^4 W}{\partial \eta^4}\right) \\
&+\left[\int_0^1\int_0^1\left(A_{11}\frac{abh^2}{2D_m}(\frac{\partial W}{\partial \zeta})^2+A_{12}\frac{a^3h^2}{2bD_m}(\frac{\partial W}{\partial \eta})^2-B_{11}\frac{abh}{D_m}\frac{\partial^2 W}{\partial \zeta^2}-B_{12}\frac{a^3h}{bD_m}\frac{\partial^2 W}{\partial^2 \eta}\right)d\zeta d\eta\right]\frac{\partial^2 W}{\partial \zeta^2} \\
&+2\left[\int_0^1\int_0^1\left(A_{66}\frac{a^3h^2}{bD_m}\frac{\partial W}{\partial \zeta}\frac{\partial W}{\partial \eta}-2B_{66}\frac{a^3h}{bD_m}\frac{\partial^2 W}{\partial \zeta \partial \eta}\right)d\zeta d\eta\right]\frac{\partial^2 W}{\partial \zeta \partial \eta} \\
&+\left[\int_0^1\int_0^1\left(A_{12}\frac{a^3h^2}{2bD_m}(\frac{\partial W}{\partial \zeta})^2+A_{22}\frac{abh^2}{2D_m}(\frac{\partial W}{\partial \eta})^2-B_{12}\frac{a^3h}{bD_m}\frac{\partial^2 W}{\partial \zeta^2}-B_{22}\frac{abh}{D_m}\frac{\partial^2 W}{\partial \eta^2}\right)d\zeta d\eta\right]\frac{\partial^2 W}{\partial \eta^2} \\
&-R_x\frac{\partial^2 W}{\partial \zeta^2}-R_y\left(\frac{a}{b}\right)^2\frac{\partial^2 W}{\partial \eta^2}+\lambda\frac{\partial W}{\partial \zeta}+\sqrt{\lambda\frac{\mu}{M}}\frac{\partial W}{\partial \tau}=0
\end{aligned}
\tag{34}
$$

## 3 DISCRETIZED FORM OF THE GOVERNING EQUATION

In this section, the governing aeroelastic equation is discretized by using the GDQM. This method implies that the $r$th-order derivative of a function $W$, at a point s = $s_i$ , with $N$ discrete points can be estimated by

$$
\left.\frac{\partial^r W}{\partial s^r}\right|_{s=s_i}=\sum_{j=1}^{N}A_{ij}^{(r)s}W_j \tag{35}
$$

The coefficient $A_{ij}^{(r)s}$ represents the weighting coefficeints. The method for constructing these coefficients can be found in Chang Shu (2000).

The DQ method may also be used for linear combinations of partial derivatives and integrals (Chang Shu, 2000) as follows:

$$\frac{\partial^{(r+s)}W}{\partial x^r \partial y^s} = \sum_{k=1}^{N}\sum_{l=1}^{M} A_{ik}^{(r)x} A_{jl}^{(s)y} W_{kl} \tag{36}$$

$$\int_0^a \int_0^b W(x,y)dxdy = \sum_{k=1}^{N}\sum_{l=1}^{M} c_k c_l W_{kl} \tag{37}$$

where $c_l, c_k$ are the weighting coefficients of the one-dimensional integral in the x and y directions respectively, and given by (Chang Shu, 2000)

$$c_k = H_{jk}^{I(x)} - H_{ik}^{I(x)} = \int_0^a r_k(x)dx \tag{38}$$

$$c_l = H_{jl}^{I(y)} - H_{il}^{I(y)} = \int_0^b r_l(y)dy \tag{39}$$

where

$$H^{I(x)} = (A^{(1)x})^{-1} \ , \ H^{I(y)} = (A^{(1)y})^{-1} \tag{40}$$

In the above equations $r_k(x)$ and $r_l(y)$ are the Lagrange interpolated polynomials. By using the DQM, the discretized form of the governing equations (Eq. 34) can be written as:

$$\begin{aligned}
&\frac{I_0}{\rho_m h}\ddot{W} + \sqrt{\lambda\frac{\mu}{M}}\dot{W} + \frac{D_{eq}}{D_m}\left(\sum_{k1=1}^{N} Ax_{ik1}^{(4)} W_{k1j} + 2\left(\frac{a}{b}\right)^2 \sum_{k1=1}^{N}\sum_{k2=1}^{M} Ay_{ik1}^{(2)} Ay_{jk2}^{(2)} W_{k1k2} + \left(\frac{a}{b}\right)^4 \sum_{k2=1}^{M} Ay_{jk2}^{(4)} W_{ik2}\right) \\
&+A_{11}\frac{abh^2}{2D_m}\sum_{k,l,m,n=1}^{N}\sum_{p=1}^{M} c_k c_p A_{kn}^{(1)x} A_{pm}^{(1)x} A_{il}^{(2)x} W_{kn} W_{pm} W_{lj} \\
&+A_{12}\frac{a^3h^2}{2bD_m}\sum_{k,l=1}^{N}\sum_{p,q,s=1}^{M} c_k c_p A_{kq}^{(1)y} A_{ps}^{(1)y} A_{il}^{(2)x} W_{kq} W_{ps} W_{lj} \\
&-B_{11}\frac{abh}{D_m}\sum_{k,l,n=1}^{N}\sum_{p=1}^{M} c_k c_p A_{kn}^{(2)x} A_{il}^{(2)x} W_{pn} W_{lj} - B_{12}\frac{a^3h}{bD_m}\sum_{k,l=1}^{N}\sum_{p,q=1}^{M} c_k c_p A_{pq}^{(2)y} A_{il}^{(2)x} W_{kq} W_{lj} \\
&+2A_{66}\frac{a^3h^2}{bD_m}\sum_{k,k1,n=1}^{N}\sum_{p,k2,q=1}^{M} c_k c_p A_{kn}^{(1)x} A_{pq}^{(1)y} A_{ik1}^{(1)x} A_{jk2}^{(1)y} W_{kn} W_{pq} W_{k1k2} \\
&-4B_{66}\frac{a^3h}{bD_m}\sum_{k,k1,n=1}^{N}\sum_{p,k2,q=1}^{M} c_k c_p A_{kn}^{(1)x} A_{pq}^{(1)y} A_{ik1}^{(1)x} A_{jk2}^{(1)y} W_{nq} W_{k1k2} \\
&+A_{12}\frac{a^3h^2}{2bD_m}\sum_{k=1}^{N}\sum_{p,q,t,s=1}^{M} c_k c_p A_{ks}^{(1)x} A_{pt}^{(1)x} A_{jq}^{(2)y} W_{ks} W_{pt} W_{iq} \\
&+A_{22}\frac{abh^2}{2D_m}\sum_{k,m,n=1}^{N}\sum_{p,q=1}^{M} c_k c_p A_{pm}^{(1)y} A_{kn}^{(1)y} A_{jq}^{(2)y} W_{pm} W_{kn} W_{iq} \\
&-B_{12}\frac{a^3h}{bD_m}\sum_{k=1}^{N}\sum_{p,q,t=1}^{M} c_k c_p A_{pt}^{(2)x} A_{jq}^{(2)y} W_{kt} W_{iq} - B_{22}\frac{abh}{D_m}\sum_{k,n=1}^{N}\sum_{p,q=1}^{M} c_k c_p A_{kn}^{(2)y} A_{jq}^{(2)y} W_{pn} W_{iq}
\end{aligned} \tag{41}$$

$$-R_x\sum_{k1=1}^{N}A_{ik1}^{(2)x}W_{k1j}-R_y\left(\frac{a}{b}\right)^4\sum_{k2=1}^{M}A_{jk2}^{(2)y}W_{ik2}+\lambda\sum_{k1=1}^{N}A_{ik}^{(1)x}W_{k1j}=0$$

$$\begin{aligned}&for\quad i,k,k,m,n,k1=1,2,...,N\\&\qquad j,p,q,s,t,k2=1,2,...,M\end{aligned}$$

Also, the assumed boundary conditions may be defined as follows:

$$\begin{aligned}&w(0,y,t)=0, \qquad \frac{\partial^2 w(0,y,t)}{\partial x^2}=0\\&w(a,y,t)=0, \qquad \frac{\partial^2 w(a,y,t)}{\partial x^2}=0\\&w(x,0,t)=0, \qquad \frac{\partial^2 w(x,0,t)}{\partial y^2}=0\\&w(x,b,t)=0, \qquad \frac{\partial^2 w(x,b,t)}{\partial y^2}=0\end{aligned} \tag{42}$$

The discretized form of these boundary conditions will be:

$$\begin{aligned}&W_{1,j}=0, \quad \sum_{k=1}^{N}A_{1,k}^{(2)x}W_{k,j}=0 \qquad at\ \zeta=0\\&W_{N,j}=0, \quad \sum_{k=1}^{N}A_{N,k}^{(2)x}W_{k,j}=0 \qquad at\ \zeta=1\\&W_{i,1}=0, \quad \sum_{k=1}^{M}A_{1,k}^{(2)x}W_{i,k}=0 \qquad at\ \eta=0\\&W_{i,M}=0, \quad \sum_{k=1}^{M}A_{M,k}^{(2)x}W_{i,k}=0 \qquad at\ \eta=0\end{aligned} \tag{43}$$

Thus, the boundary conditions can be written as:

$$\begin{aligned}&\sum_{k=2}^{N-1}A_{1,k}^{(2)x}W_{k,j}=0\\&\sum_{k=2}^{N-1}A_{N,k}^{(2)x}W_{k,j}=0\\&\sum_{k=2}^{M-1}A_{1,k}^{(2)x}W_{i,k}=0\\&\sum_{k=2}^{M-1}A_{M,k}^{(2)x}W_{i,k}=0\end{aligned} \tag{44}$$

By incorporating the boundary conditions into Eq. (41) and doing some manipulations, the final aerothermoelastic equation of a FG plate can be drawn as:

$$\begin{aligned}
&\frac{I_0}{\rho_m h}\ddot{W}+\sqrt{\lambda\frac{\mu}{M}}\,\dot{W}+\frac{D_{eq}}{D_m}\left(\sum_{k=3}^{N-2}C_1W_{kj}+2\left(\frac{a}{b}\right)^2\sum_{k1=3}^{N-2}\sum_{k2=3}^{M-2}C_2W_{k1k2}+\left(\frac{a}{b}\right)^4\sum_{k=3}^{M-2}C_3W_{ik}\right)\\
&+A_{11}\frac{abh^2}{2D_m}\sum_{k,l,m,n=3}^{N-2}\sum_{p=3}^{M-2}C_4W_{kn}W_{pm}W_{lj}+A_{12}\frac{a^3h^2}{2bD_m}\sum_{k,l=3}^{N-2}\sum_{m,n,p=3}^{M-2}C_5W_{kp}W_{mn}W_{lj}\\
&-B_{11}\frac{abh}{D_m}\sum_{k,l,n=3}^{N-2}\sum_{p=3}^{M-2}C_6W_{pn}W_{lj}-B_{12}\frac{a^3h}{bD_m}\sum_{k,l=3}^{N-2}\sum_{p,q=3}^{M-2}C_7W_{kq}W_{lj}\\
&+2A_{66}\frac{a^3h^2}{bD_m}\sum_{k,k1,n=3}^{N-2}\sum_{p,k2,q=3}^{M-2}C_8W_{kn}W_{pq}W_{k1k2}-4B_{66}\frac{a^3h}{bD_m}\sum_{k,k1,n=3}^{N-2}\sum_{p,k2,q=3}^{M-2}C_9W_{nq}W_{k1k2}\\
&+A_{12}\frac{a^3h^2}{2bD_m}\sum_{k=3}^{N-2}\sum_{p,q,t,s=3}^{M-2}C_{10}W_{ks}W_{pt}W_{iq}+A_{22}\frac{abh^2}{2D_m}\sum_{k,m,n=3}^{N-2}\sum_{p,q=3}^{M-2}C_{11}W_{pm}W_{kn}W_{iq}\\
&-B_{12}\frac{a^3h}{bD_m}\sum_{k=3}^{N-2}\sum_{p,q,t=3}^{M-2}C_{12}W_{kt}W_{iq}-B_{22}\frac{abh}{D_m}\sum_{k,n=3}^{N-2}\sum_{p,q=3}^{M-2}C_{13}W_{pn}W_{iq}-R_x\sum_{k=3}^{N-2}C_{14}W_{kj}\\
&-R_y\left(\frac{a}{b}\right)^4\sum_{k=3}^{M-2}C_{15}W_{ik}+\lambda\sum_{k=3}^{N-2}C_{16}W_{kj}=0
\end{aligned}\tag{45}$$

$$\begin{aligned}
&for\quad i,k,k,m,n,k1=3,4,...,N-2\\
&\qquad j,p,q,s,t,k2=3,4,...,M-2
\end{aligned}$$

where $C_1$ to $C_{16}$ are defined in Appendix A

## 4 RESULTS AND DISCUSSION

In this section, the critical dynamic pressures for FG plates are calculated to investigate the validity of the GDQM for determining flutter boundaries. In this regard, a simply-supported functionally graded flat plate made of a combination of metal (SUS304) and ceramic ($Si_3N_3$) is considered as a test case. The material properties are listed in Table 1 (Navazi and Haddadpour, 2011).

In order to obtain the flutter instability, the governing aerothermoelastic equation (Eq. 45) is utilized by considering 11 × 11 sampleing points in the computational domain. However, after some investigations, it was found that the present nonlinear analysis is extremely sensitive to the sampling point distribution. Thus, Chebyshev-Gauss-Lobatto distribution is not a right choice for this type of problems, but the suggested distribution by Tomasiello (1998) can be used as an alternative choice. Then, the resulting ordinary differential equations are solved via the 4th order Runge-Kutta method.

| Material | Young's modulus (GPa) | Poisson's ratio | Mass density ($Kg/m^3$) | CTE (1/K) | Thermal conductivity (W/mK) |
|---|---|---|---|---|---|
| SUS304 | 207.8 | 0.3 | 7800 | 1.53E-05 | 1.214E+01 |
| $Si_3N_3$ | 322.3 | 0.3 | 3200 | 7.47E-06 | 1.011E+01 |

**Table 1**: Material properties at reference temperature (T= 300 K)

Table 2 shows the obtained critical non-dimensional dynamic pressures ($\lambda_{cr}$) of a FG square plate with $a/b$=1(aspect ratio), $a/h$=100 (length/ thickness ratio) along with those reported by Sohn and Kim (2008) under different volume fractions and temperatures. It is clear that the obtained results are in good agreement with Sohn and Kim (2008).

| Temperature changes of the surfaces | Volume fraction | $\lambda_{cr}$ Present | $\lambda_{cr}$ Sohn and Kim (2008) | Error (%) |
|---|---|---|---|---|
| $T_m$=300 | n=0.0 | 792.81 | 792.70 | 0.012 |
| $T_c$=300 | n=0.5 | 682.50 | 681.40 | 0.161 |
| | n=1 | 642.82 | 641.30 | 0.233 |
| | n=5 | 586.25 | 584.90 | 0.230 |
| | n=∞ | 512.13 | 511.10 | 0.195 |
| $T_m$=300 | n=0.0 | 713.90 | 715.80 | 0.265 |
| $T_c$=310 | n=0.5 | 598.32 | 599.00 | 0.116 |
| | n=1 | 554.85 | 555.40 | 0.099 |
| | n=5 | 489.10 | 491.90 | 0.569 |
| | n=∞ | 408.45 | 414.80 | 1.530 |
| $T_m$=310 | n=0.0 | 636.80 | 638.3 | 0.234 |
| $T_c$=310 | n=0.5 | 501.45 | 503.4 | 0.387 |
| | n=1 | 454.23 | 454.9 | 0.147 |
| | n=5 | 387.52 | 388.5 | 0.252 |
| | n=∞ | 311.25 | 312.0 | 0.240 |

**Table 2**: Critical non-dimensional dynamic pressure

Next, to validate the post flutter characteristics of the present computational model, the limit cycle amplitudes of an isotropic square panel for various dynamic pressures, at a specified location ($\zeta = 0.75$ and $\eta = 0.5$) on the panel are computed and depicted in Fig. 1. As is evident, the DQM results are in satisfactory agreement with those presented by Dowell (1966) and Xue and Mei (1993) which used time integration and finite element method, respectively.

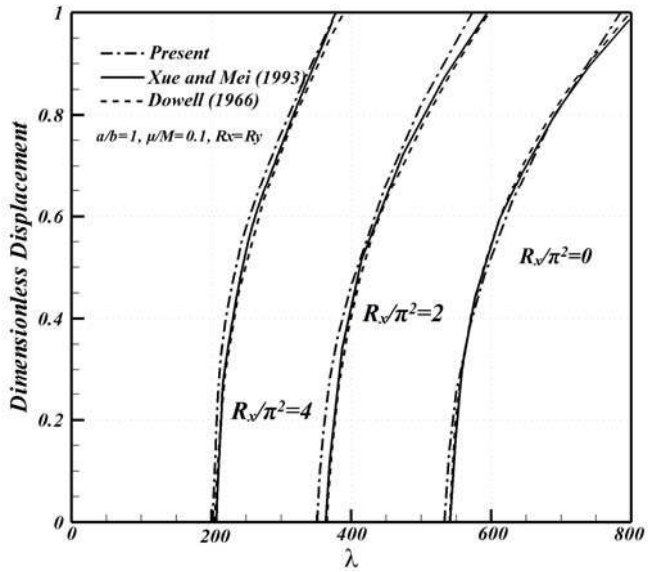


**Figure 1**: LCO amplitudes of the isotropic square panel

Finally, the aerothermoelastic stability boundaries of the panel according to in-plane thermal load are depicted in Fig. 2. As shown in this figure, the developed tool can capture different dynamic behaviors of the plate, including stable, limit cycle oscillation (LCO), Buckled and chaotic, as well as Xue and Mei (1993).

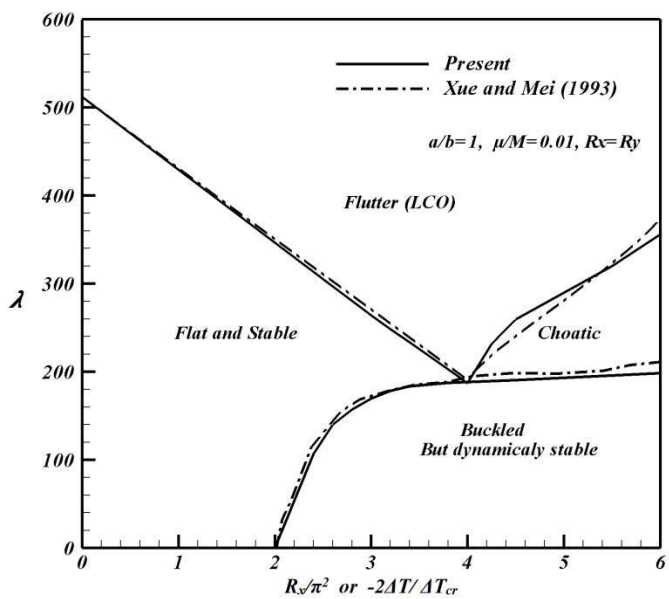


**Figure 2**: Stability boundaries of the isotropic square panel

Fig. 3 shows the critical dynamic pressure of the aforementioned FG panel versus volume fraction index ($n$). It can be seen that as $\mu/M$ decreases the critical dynamic pressure decreases too. On

the other hand, any increase in volume fraction index leads to reduction in the critical dynamic pressure. However, this reduction is impressive until the value of volume fraction becomes about unity.

The effects of aspect ratio $(a/b)$ on the critical dynamic pressure are presented in Fig. 4. It can be seen that the critical dynamic pressure increases with the plate aspect ratio. Moreover, the variation of critical dynamic pressure with respect to $\mu/M$ is more dominant for plates with higher aspect ratio.

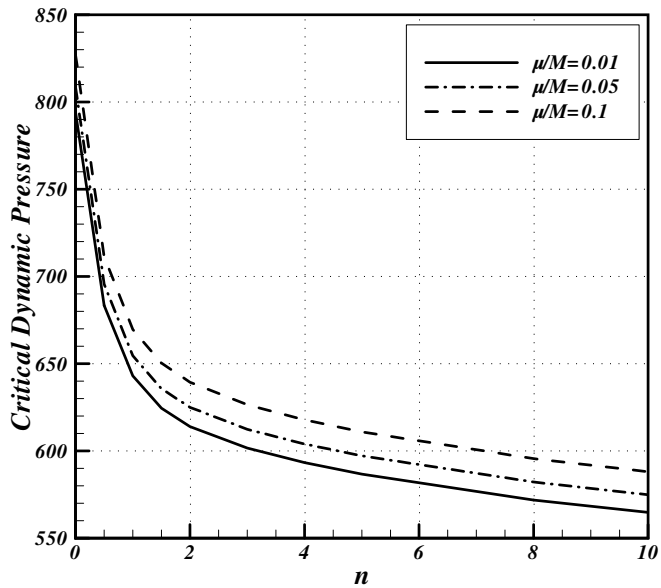


**Figure 3**: Effect of $\mu/M$ on the critical dynamic pressure of the FG panel $(a/h{=}100)$

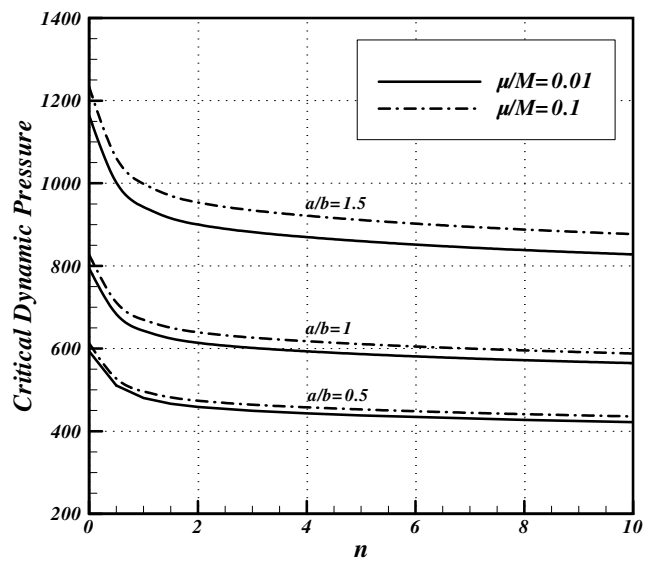


**Figure 4**: Effect of aspect ratio on the critical dynamic pressure of the FG panel $(a/h{=}100)$

The limit cycle amplitude of the FG plate at the aforementioned point versus the critical dynamic pressure for various volume fraction indexes and different values of $T_c$ is shown in Figure 5. It should be noted that the value of $T_c$ is considerd to vary from 300 K (the gary lines) to 320 K (the black lines) and Tm is taken to be 300 K. It is found that by increasing the surface temperature of the FG plate, the critical dynamic pressure is decreased.

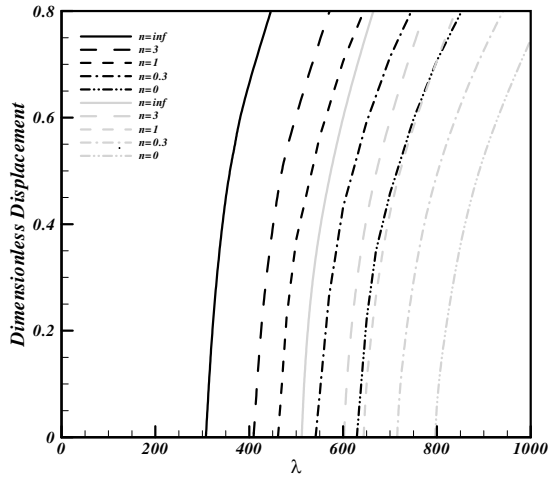


**Figure 5**: Deflection LCO dimensionless amplitude of the FG panel.

The aerothermoelastic stability margins versus in-plane thermal load for various volume fraction indexes are shown in Fig. 6. It can be seen that as the volume fraction index decreases the critical thermal buckling load, the critical dynamic pressure and the in-plane thermal load, where the chaotic motion begins, all increase. As a result, the bifurcation point shifts to the top right.

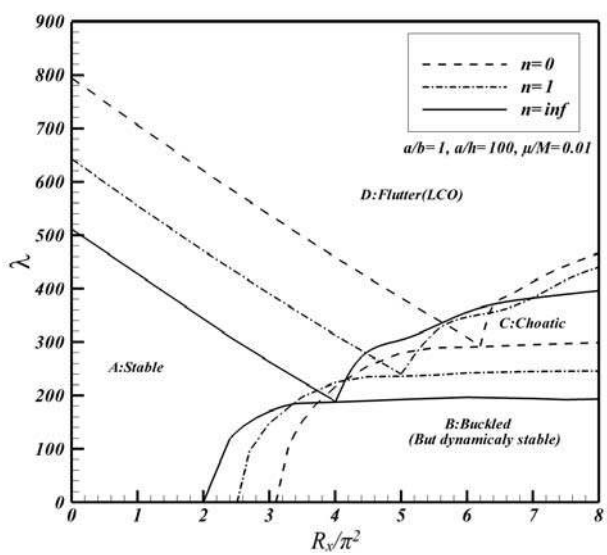


**Figure 6**: Stability boundaries of the FG panel at various n

As shown in Fig. 6, the plate remains stable in zone A. The typical time history of this zone is shown in Fig. 7.

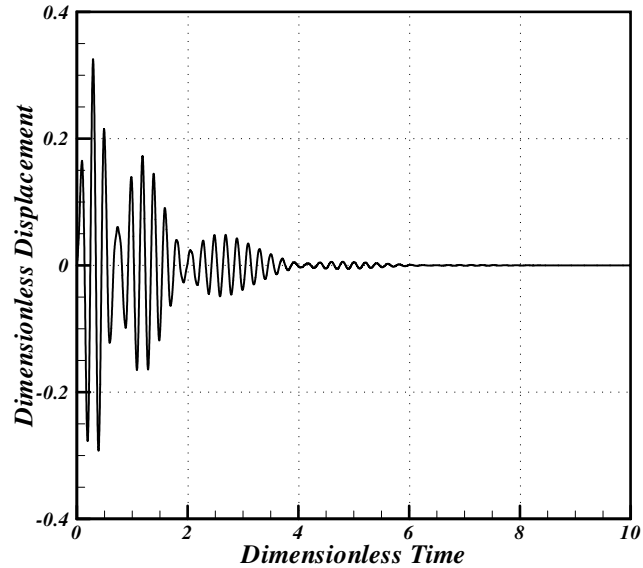


**Figure 7**: Non-dimensional deflection of the panel ($\lambda$=350, $n$=1, $R_x$=$R_y$=$3\pi^2$)

In zone B, the panel is dynamically stable, but statically unstable and buckled. The dimensionless deflection time histories in zone B for two specific conditions are shown in Figs. 8 and 9. They reveal that the steady response of the panel increases with increasing of $n$. They also show that the amplitude of the panel motion decreases with increasing of dynamic pressure.

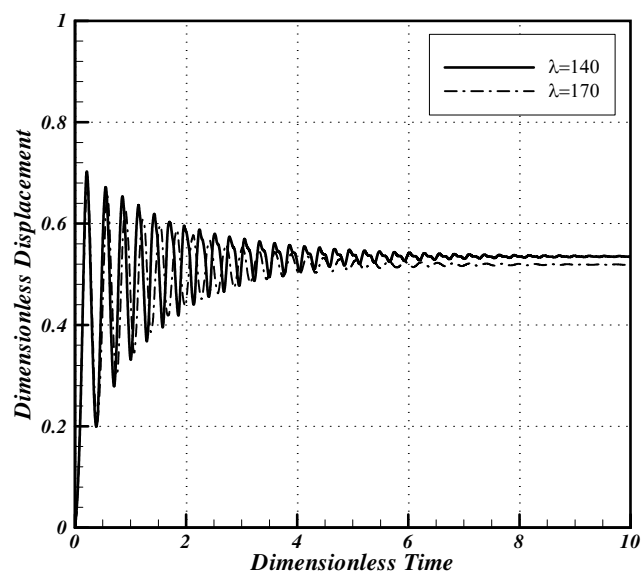


**Figure 8**: Non-dimensional deflection of the panel ($n$=0, $R_x$=$R_y$=$5\pi^2$)

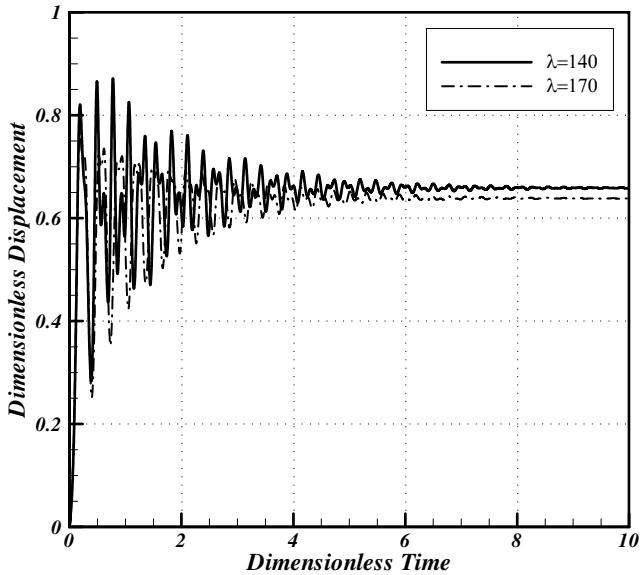


**Figure 9**: Non-dimensional deflection of the panel ($n$=1, $R_x$=$R_y$=$5\pi^2$)

At zone C the plate motion is chaotic and the time history response and the related phase diagram at a specified condition ($\lambda$=420, $n$=0, $R_x$=$R_y$=$8\pi^2$ is shown in Figs. 10 and 11, respectively.

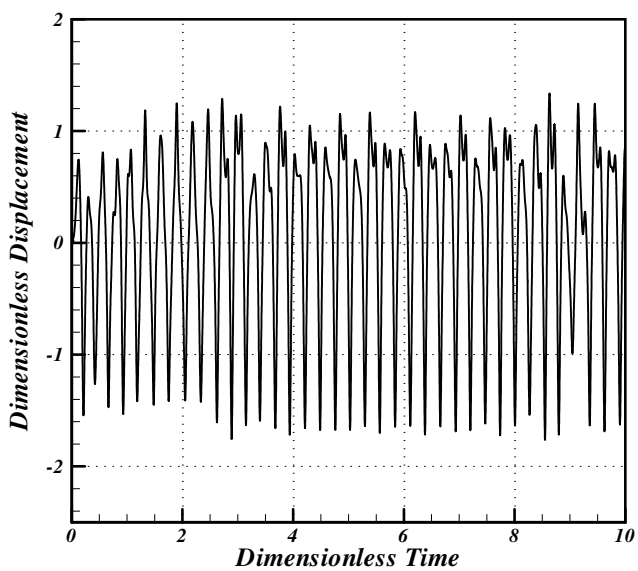


**Figure 10**: chaotic time history of the panel ($\lambda$=420, $n$=0, $R_x$=$R_y$=$8\pi^2$)

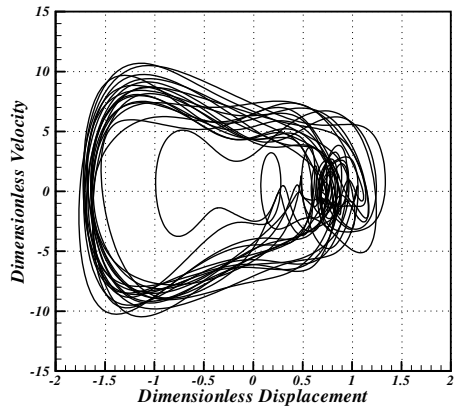


**Figure 11**: Phase plane of the chaotic motion ($\lambda$=420, $n$=0, $R_x$=$R_y$=$8\pi^2$)

As mentioned before, the limit cycle oscillation occurs in zone D. The deflection time history and the related phase diagram in this zone for two specified conditions are shown in Figs. 12 to 15. However, for moderate $R_x$ as dynamic pressure increases, the periodic limit cycle oscillation changes to the simple harmonic limit cycle oscillation.

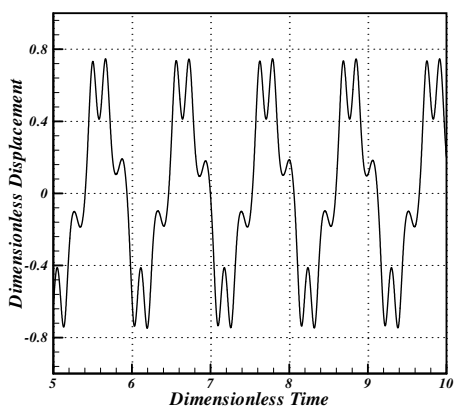


**Figure 12**: Time history of the panel ($\lambda$=195, $n$=$\infty$, $R_x$=$R_y$=$4\pi^2$)

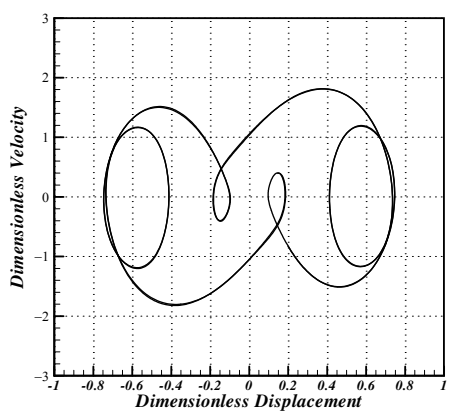


**Figure 13**: Phase plane ($\lambda$=195, $n$=*inf*, $R_x$=$R_y$=$4\pi^2$)

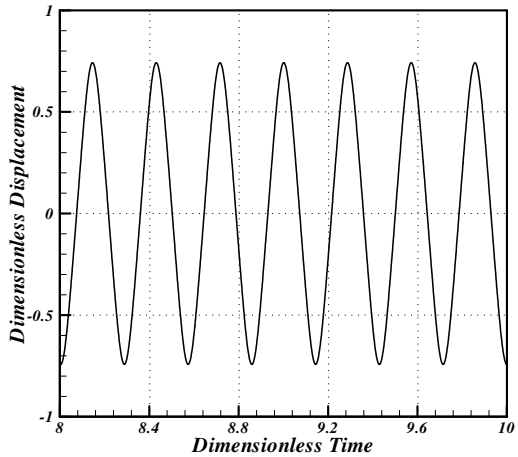


**Figure 14**: Non-dimensional deflection ($\lambda$=280,$n$=*inf*, $R_x$=$R_y$=$4\pi^2$)

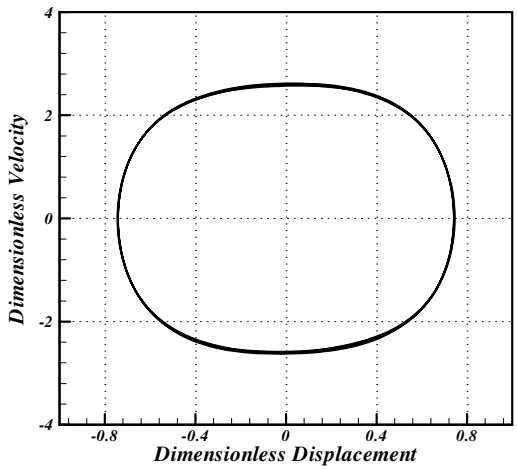


**Figure 15**: Phase plane ($\lambda$=280, $n$=*inf*, $R_x$=$R_y$=$4\pi^2$)

## 5 CONCLUSIONS

In this study, the GDQM has been used to provide the ordinary differential form of the aerothermoelastic equation of a FG flat plate. To investigate the aerothermoelastic behavior of the plate, the $4^{th}$ order Runge-Kutta numerical method has been utilized. The evaluation of the obtained results in comparison with those available in literature shows the accuracy and ability of the GDQM to study the aerothermoelastic behavior of a FG panel in supersonic regime. However, it should be noted that the application of this method is much simpler than other well-known computational methods such as (Galerkin, and FEM). Also, it was found that the nonlinear panel flutter analysis with GDQM is extremely sensitive to the grid point distribution. Therefore, the well-known Chebyshev-Gauss-Lobatto distribution is not suitable for this type of problems, but Tomasiello's distribution (Tomasiello, 1998) can be suggested as an efficient and suitable choice.

Finally, this study reveals that increasing of the surface temperature of a FG plate leads to decrease in the critical dynamic pressure due to the reduction of structural Rigidity. Also, it has been shown that some parameters such as volume fraction index, Mach number, in-plane thermal load and plate aspect ratio were found to have significant effects on the aeroelastic behavior or dynamical motion of a FG plate.

## References

B.A. Miller, J.J. McNamara, S.M. Spottswood, A.J. Culler, The impact of flow induced loads on snap-through behavior of acoustically excited, thermally buckled panels. Journal of Sound and Vibration 2011; 330:5736–5752.

Bellman, R.E., Casti, J., (1971). Differential quadrature and long-term integration. J. Math. Anal. Appl. 34, 235–238

Bert, C.W., Jang, S.K., Striz, A.G., (1988). Two new approximate methods for analyzing free vibration of structural components. AIAA J. 26, 612–618

Bert, C.W., Jang, S.K., Striz, A.G., (1989). Nonlinear bending analysis of orthotropic rectangular plates by themethod of differential quadrature. Comput. Mech. 5, 217–226

Bert, C.W., Malik, M., (1996). Differential quadrature in computational mechanics: a review. Appl. Mech. Rev. 49, 1–27

Bolotin, V. V., (1963). Non-conservative Problems of the Theory of Elastic Stability, Mcmillan, New York 199-312.

Dowell EH., (1966). Nonlinear oscillations of a fluttering plate. I. AIAA J 4(7):1267–75.

Dowell, E. H., (1975). Aeroelasticity of Plates and Shells, Noordhoff Internationla Publishing, Leyden.

H.M. Navazi, H. Haddadpour., (2011). Nonlinear aero-thermoelastic analysis of homogeneous and functionally graded plates in supersonic airflow using coupled models. Comp Struct 93:2554-65

Houbolt, J. C., (1958). A Study of Several Aerothermoelastic Problems of Aircraft Structures in High Speed Flight,PhD. Thesis, No. 2760, Swiss Federal Institute of Technology, Zurich, Switzerland.

Javaheri R, Eslami MR., (2002). Thermal buckling of functionally graded plates. AIAA J 40(1):162–9.

K.-J. Sohn, J.-H. Kim., (2008). Structural stability of functionally graded panels subjected to aero-thermal loads. Comp Struct 82:317-25

K.-J. Sohn, J.-H. Kim., (2009). Nonlinear thermal flutter of functionally graded panels under a supersonic flow. Comp Struct 88:380-87

Liaw, D.G., Yang, T.Y., (1993). Reliability and nonlinear supersonic flutter of uncertain laminated plates. AIAA J. 31(12), 2304–2311.

M. Talebitooti, R. Talebitooti, K. Daneshjou, H. Saeidi Googarchin, (2013). Dynamic Analysis and Critical Speed of Rotating Laminated Conical Shells with Orthogonal Stiffeners. Latin American Journal of Solids and Structures10: 349 – 390

M.N.A. Gulshan Taj, and Anupam Chakrabarti, (2013). Dynamic analysis of functionally graded skew shell panel, Latin American J. of Solids and Struct., vol.10, no.6, pp., 1243-1266.

Maziar Janghorban, and Amin Zare, (2011). Thermal effect on free vibration analysis of functionally graded arbitrary straight-sided plates with different cutouts," Latin Americal J. Solids and Struct., vol.8, pp. 245–257.

Mei C, Abdel-Moltagaly K, Chen R., (1999). Review of nonlinear panel flutter at supersonic and hypersonic speeds. Appl Mech Rev 52(10):321–32.

Miyamoto Y, Kaysser WA, Rabin BH, Kawasaki A, Ford RG. (1999). Functionally graded materials: design, processing and applications. Kluwer Academic Publishers p. 1–6.

Praveen, G. N., and Reddy, J. N., (1998). Nonlinear Transient Thermoelastic Analysis of Functionally Graded Ceramic-Metal Plates,Int. J.Solids Struc., 72(1),10-18.

S. A. Fazelzadeh, P. Malekzadeh, P. Zahedinejad, and M. Hosseini, (2007). Vibration Analysis of Functionally Graded Thin-Walled Rotating Blades Under High Temperature Supersonic Gas Flow Using the DQM, Journal of Sound and Vibration, vol. 306, nos. 1–2, pp. 333–348.

Shaeffer HG, Heard Jr WL., (1965). Flutter of a flat panel subjected to nonlinear temperature distribution. AIAA J 30(10) : 1918-23

Shu, C., Richards, B.E., (1992). Application of generalized differential quadrature to solve two-dimensional incompressible Navier-Stoaks equations. Int. J. Numer. Meth. Fluids 15, 791–798

Shu, C., Wang, C.M., (1999). Treatment of mixed and non-uniform boundary conditions in GDQ vibration analysis of rectangular plate, Eng. Struct. 21, 125–134

Shu, Chang, (2000). Differential Quadrature and It's Application in Engineering, Springer-Verlag London Limited.

Tomasiello, S., (1998). Differential Quadrature Method: Application to Initial-Boundary-Value Problems, J. of Sound and Vibration 218(4), 573-585.

Xue DY, Mei C., (1993a). Finite element nonlinear panel flutter with arbitrary temperatures in supersonic flow. AIAA J 31(1):154–62.

Xue DY, Mei C., (1993b). Finite element nonlinear flutter and fatigue life of two-dimensional panels with temperature effects. J Aircraft 30(6): 993–1000.

## Appendix A

The $C_i$ coefficients in Eq. (45) are defined through the following relations:

$$C_1 = A_{ik}^{(4)x} - \frac{A_{i,2}^{(4)x}.AXK1 + A_{i.N-1}^{(4)x}AXKN}{AXN}$$

$$C_2 = (A_{ik1}^{(2)x} - \frac{A_{i,2}^{(2)x}.AXK1 + A_{i.N-1}^{(2)x}AXKN}{AXN})(A_{jk2}^{(2)y} - \frac{A_{j,2}^{(2)y}.AYK1 + A_{j.M-1}^{(2)y}AYKM}{AYM})$$

$$C_3 = (A_{jk}^{(4)y} - \frac{A_{j,2}^{(4)y}.AYK1 + A_{j.M-1}^{(4)y}AYKM}{AYM})$$

$$C_4 = c_k c_p (A_{kn}^{(1)x} - \frac{A_{k,2}^{(1)x}.AXK1 + A_{k.N-1}^{(1)x}AXKN}{AXN})(A_{pm}^{(1)x} - \frac{A_{p,2}^{(1)x}.AXK1 + A_{p.N-1}^{(1)x}AXKN}{AXN})$$
$$(A_{il}^{(2)x} - \frac{A_{i,2}^{(2)x}.AXK1 + A_{i.N-1}^{(2)x}AXKN}{AXN})$$

$$C_5 = c_k c_p (A_{kq}^{(1)y} - \frac{A_{k,2}^{(1)y}.AYK1 + A_{k.M-1}^{(1)y}AYKM}{AYM})(A_{ps}^{(1)y} - \frac{A_{p,2}^{(1)y}.AYK1 + A_{p,M-1}^{(1)y}AYKM}{AYM})$$
$$(A_{il}^{(2)x} - \frac{A_{i,2}^{(2)x}.AXK1 + A_{i.N-1}^{(2)x}AXKN}{AXN})$$

$$C_6 = c_k c_p (A_{kn}^{(2)x} - \frac{A_{k,2}^{(2)x}.AXK1 + A_{k.N-1}^{(2)x}AXKN}{AXN})(A_{il}^{(2)x} - \frac{A_{i,2}^{(2)x}.AXK1 + A_{i.N-1}^{(2)x}AXKN}{AXN})$$

$$C_7 = c_k c_p (A_{pq}^{(2)y} - \frac{A_{p,2}^{(2)y}.AYK1 + A_{p,M-1}^{(2)y}AYKM}{AYM})(A_{il}^{(2)x} - \frac{A_{i,2}^{(2)x}.AXK1 + A_{i.N-1}^{(2)x}AXKN}{AXN})$$

$$C_8 = c_k c_p (A_{kn}^{(1)x} - \frac{A_{k,2}^{(1)x}.AXK1 + A_{k.N-1}^{(1)x} AXKN}{AXN})(A_{pq}^{(1)y} - \frac{A_{p,2}^{(1)y}.AYK1 + A_{p.M-1}^{(1)y} AYKM}{AYM})$$
$$(A_{ik1}^{(1)x} - \frac{A_{i,2}^{(1)x}.AXK1 + A_{i.N-1}^{(1)x} AXKN}{AXN})(A_{jk2}^{(1)y} - \frac{A_{j,2}^{(1)y}.AYK1 + A_{j.M-1}^{(1)y} AYKM}{AYM})$$

$$C_9 = c_k c_p (A_{ks}^{(1)x} - \frac{A_{k,2}^{(1)x}.AXK1 + A_{k.N-1}^{(1)x} AXKN}{AXN})(A_{pt}^{(1)y} - \frac{A_{p,2}^{(1)y}.AYK1 + A_{p.M-1}^{(1)y} AYKM}{AYM})$$
$$(A_{ik1}^{(1)x} - \frac{A_{i,2}^{(1)x}.AXK1 + A_{i.N-1}^{(1)x} AXKN}{AXN})(A_{jk2}^{(1)y} - \frac{A_{j,2}^{(1)y}.AYK1 + A_{j.M-1}^{(1)y} AYKM}{AYM})$$

$$C_{10} = c_k c_p (A_{ks}^{(1)x} - \frac{A_{k,2}^{(1)x}.AXK1 + A_{k.N-1}^{(1)x} AXKN}{AXN})(A_{pt}^{(1)x} - \frac{A_{p,2}^{(1)x}.AXK1 + A_{p.N-1}^{(1)x} AXKN}{AXN})$$
$$(A_{jq}^{(1)y} - \frac{A_{j,2}^{(1)y}.AYK1 + A_{j,M-1}^{(1)y} AYKM}{AYM})$$

$$C_{11} = c_k c_p (A_{pm}^{(1)y} - \frac{A_{p,2}^{(1)y}.AYK1 + A_{p,M-1}^{(1)y} AYKM}{AYM})(A_{kn}^{(1)y} - \frac{A_{k,2}^{(1)y}.AYK1 + A_{k,M-1}^{(1)y} AYKM}{AYM})$$
$$(A_{jq}^{(2)y} - \frac{A_{j,2}^{(2)y}.AYK1 + A_{j,M-1}^{(2)y} AYKM}{AYM})$$

$$C_{12} = c_k c_p (A_{pt}^{(2)x} - \frac{A_{p,2}^{(2)x}.AXK1 + A_{p,N-1}^{(2)x} AXKN}{AXN})(A_{jq}^{(2)y} - \frac{A_{j,2}^{(2)y}.AYK1 + A_{j,M-1}^{(2)y} AYKM}{AYM})$$

$$C_{13} = c_k c_p (A_{kn}^{(2)y} - \frac{A_{k,2}^{(2)y}.AYK1 + A_{k,M-1}^{(2)y} AYKM}{AYM})(A_{jq}^{(2)y} - \frac{A_{j,2}^{(2)y}.AYK1 + A_{j,M-1}^{(2)y} AYKM}{AYM})$$

$$C_{14} = (A_{ik}^{(2)x} - \frac{A_{i,2}^{(2)x}.AXK1 + A_{i,N-1}^{(2)x} AXKN}{AXN})$$

$$C_{15} = (A_{jk}^{(2)y} - \frac{A_{j,2}^{(2)y}.AYK1 + A_{j,M-1}^{(2)y} AYKM}{AYM})$$

$$C_{16} = (A_{ik}^{(1)x} - \frac{A_{i,2}^{(1)x}.AXK1 + A_{i,N-1}^{(1)x} AXKN}{AXN})$$

Where

$$AXN = A_{N,2}^{(2)x}.A_{1,N-1}^{(2)x} - A_{1,2}^{(2)x}.A_{N,N-1}^{(2)x}$$
$$AXK1 = A_{1,k}^{(2)x}.A_{N,N-1}^{(2)x} - A_{1,N-1}^{(2)x}.A_{N,k}^{(2)x}$$
$$AXKN = A_{1,2}^{(2)x}.A_{N,k}^{(2)x} - A_{1,k}^{(2)x}.A_{N,2}^{(2)x}$$
$$AYN = A_{M,2}^{(2)y}.A_{1,M-1}^{(2)y} - A_{1,2}^{(2)y}.A_{M,M-1}^{(2)y}$$
$$AYK1 = A_{1,k}^{(2)y}.A_{M,M-1}^{(2)y} - A_{1,M-1}^{(2)y}.A_{M,k}^{(2)y}$$
$$AYKN = A_{1,2}^{(2)y}.A_{M,k}^{(2)y} - A_{1,k}^{(2)y}.A_{M,2}^{(2)y}$$